N-64-10335

S 70806
32p,s

NASA TECHNICAL NOTE

NASA TN D-2042

NASA TN D-2042

EFFECT OF AFTERBODY GEOMETRY AND STING DIAMETER ON THE AERODYNAMIC CHARACTERISTICS OF SLENDER BODIES AT MACH NUMBERS FROM 1.57 TO 2.86

by Dennis E. Fuller and Victor E. Langhans

Langley Research Center
Langley Station, Hampton, Va.

NATIONAL AERONAUTICS AND SPACE ADMINISTRATION • WASHINGTON, D. C. • NOVEMBER 1963

TECHNICAL NOTE D-2042

EFFECT OF AFTERBODY GEOMETRY AND STING DIAMETER ON THE AERODYNAMIC CHARACTERISTICS OF SLENDER BODIES AT MACH NUMBERS FROM 1.57 TO 2.86

By Dennis E. Fuller and Victor E. Langhans

Langley Research Center
Langley Station, Hampton, Va.

NATIONAL AERONAUTICS AND SPACE ADMINISTRATION

EFFECT OF AFTERBODY GEOMETRY AND STING DIAMETER ON THE AERODYNAMIC CHARACTERISTICS OF SLENDER BODIES AT MACH NUMBERS FROM 1.57 TO 2.86

By Dennis E. Fuller and Victor E. Langhans

SUMMARY

An investigation has been made in the low Mach number test section of the Langley Unitary Plan wind tunnel to determine the effects of afterbody boattail, camber, and length, and of variations in sting diameter on the aerodynamic characteristics of slender bodies. A common forebody was utilized for all configurations tested. Tests were performed at Mach numbers from 1.57 to 2.86 and at a Reynolds number per foot of 3.0×10^6.

The results indicate that wind-tunnel models of airplanes with afterbodies which are appreciably altered to accommodate a rear-mounted sting-support system will produce different drag characteristics than those which would be obtained from true representations of the aircraft with closed afterbodies. It is further indicated that negative afterbody camber may be beneficial in minimizing the trim performance penalty of airplanes. There is little effect of sting diameter on the aerodynamic characteristics in pitch of the wind-tunnel models that have turbulent flow over their length. There is, in general, little variation in the base-pressure coefficients with angles of attack from -4° to 4°.

INTRODUCTION

Wind-tunnel tests of airplane models generally require distortion of the model afterbody in order to permit installation of the sting-support strut and instrumentation. With the current and anticipated development of high-performance supersonic aircraft it becomes increasingly important that the effects of model afterbody distortion be known so that a more accurate definition of full-scale performance characteristics may be obtained from results of wind-tunnel model tests.

The investigation of reference 1 provided drag information on the effects of variation in sting size, and limited effects of afterbody boattailing at zero angle of attack. These tests were limited to a few configurations at a Mach number of 1.5. In an attempt to define more clearly the effects of afterbody configuration over a range of supersonic Mach numbers, the present investigation was undertaken with a series of afterbodies which varied in boattail angle, camber,

and length. The effect of varying sting diameter was also investigated. The tests were performed in the Langley Unitary Plan wind tunnel at Mach numbers from 1.57 to 2.86 through an angle-of-attack range from about -4° to 4°. The Reynolds number of the tests was about 3.0×10^6 per foot.

SYMBOLS

The coefficients of forces and moments are referred to the stability axis system. For all models, the aerodynamic moments were taken about a point located 15.01 inches aft of the nose.

A	body reference area, 0.049038 sq ft
C_D	drag coefficient, $\frac{\text{Drag}}{qA}$
$C_{D,min}$	minimum drag coefficient
$C_{D,c}$	chamber drag coefficient, $\frac{\text{Chamber drag}}{qA}$
C_L	lift coefficient, $\frac{\text{Lift}}{qA}$
C_{L_α}	slope of lift curve at $\alpha = 0^{\circ}$, $\frac{\partial C_L}{\partial \alpha}$, per deg
$\Delta C_{L,o}$	incremental C_L at $\alpha = 0^{\circ}$ between a given body and body I-4
C_m	pitching-moment coefficient, $\frac{\text{Pitching moment}}{qAd}$
C_{m_α}	slope of pitching-moment curve at $\alpha = 0^{\circ}$, $\frac{\partial C_m}{\partial \alpha}$, per deg
$\Delta C_{m,o}$	incremental C_m at $\alpha = 0^{\circ}$ between a given body and body I-4
C_p	pressure coefficient
d	exit diameter of afterbody
d_{max}	maximum body diameter, 3.00 in.
M	free-stream Mach number

p_t stagnation pressure, lb/sq in.

q free-stream dynamic pressure, lb/sq ft

T_t stagnation temperature, $^{\circ}F$

α angle of attack of fuselage center line, deg

APPARATUS AND TESTS

Wind Tunnel

Tests were conducted in the low Mach number test section of the Langley Unitary Plan wind tunnel which is a variable-pressure continuous-flow tunnel. The test section is approximately 4 feet square and 7 feet long. The nozzle leading to the test section is of the asymmetric sliding-block type which permits a continuous variation in test-section Mach number from about 1.5 to 2.9.

Models

A dimensional drawing of the models is presented in figure 1, and a photograph of one of the models and its support system is presented as figure 2. The forebody used for all the models consisted of a conical ogive nose 15 inches in length which was faired into a 3-inch-diameter cylindrical section 5 inches in length. Two families of afterbodies were tested, consisting of seven afterbodies 14.50 inches in length, and three afterbodies 19.00 inches in length. Hereinafter the afterbody designations shown in figure 1 will be used for purposes of identification of the various configurations.

Configurations I-1 through I-4 are models with afterbody boattailing, varying from a cylinder to a symmetrical ogive. Configurations I-4 through I-6 are cambered afterbody models varying from a symmetrical ogive (I-4) to a cambered ogive with a $1\frac{1}{2}$-inch offset at the rear (I-6). Configuration I-7 is a model with a conical afterbody. The three configurations with 19.00-inch afterbodies are: II-1, a cylinder; II-2, partially closed ogive comparable to configuration I-2; and II-4, a symmetrical ogive comparable to configuration I-4.

All configurations were strut supported from the bottom (see fig. 2), and thus allowed various cylindrical stings to be inserted from the rear without contacting the model. Stings with diameters of 0.75, 1.50, and 2.25 inches were used where applicable.

Test Conditions

Tests were performed at the following conditions:

M	T_t, °F	p_t, lb/sq in. abs
1.57	125	11.17
2.16	125	13.98
2.50	150	17.67
2.86	150	21.35

The Reynolds number was constant at 3.0×10^6 per foot.

The dewpoint, measured at stagnation pressure, was maintained below -30° F to assure negligible condensation effects. The angle of attack was varied from approximately -4° to 4° and the sideslip angle was maintained near 0°. In order to assure turbulent flow over the length of the body, a $\frac{1}{16}$-inch-wide strip of No. 60 carborundum grit was fixed around the nose of the model $\frac{15}{16}$ inch aft of the tip.

The aerodynamic forces and moments were measured by means of an internally mounted strain-gage balance which was, in turn, rigidly fastened to a bottom-mounted strut support, and thence to the tunnel support system.

Balance chamber pressure was measured by means of orifices located in the rear of each open-end afterbody.

Corrections and Accuracy

Angles of attack have been corrected for deflection of sting and balance due to aerodynamic loads.

The drag coefficients presented have been adjusted to correspond to free-stream static pressure acting over the base. Variation of chamber drag coefficients with angle of attack is presented in figure 3. No attempt was made to apply corrections for flow angularity to the data presented herein because of the undefined effects of the support strut on the flow over the afterbodies.

Based upon calibrations and repeatability of data, it is estimated that the various measured quantities are accurate within the following limits:

M . . . . . ±0.015
α, deg . . . . . ±0.10
$C_{D,c}$ . . . . . ±0.009

C_D . . . . . ±0.001
C_L . . . . . ±0.008
C_m . . . . . ±0.01

RESULTS AND DISCUSSION

Sting Effects

The effects of sting diameter on the aerodynamic characteristics in pitch of a cylindrical afterbody (I-1) configuration and two afterbody configurations with different degrees of boattailing (I-2 and I-3) indicate that within the accuracy of these tests, there are no appreciable effects of sting diameter on the aerodynamic characteristics in pitch of any of the test configurations through the test Mach number range. (See fig. 4.) The drag coefficient results are in agreement with the data of reference 1 (M = 1.5, only) which concluded that the base or chamber drag coefficient of a symmetrical body with turbulent flow over its length is the only parameter affected by change in sting diameter.

Afterbody Boattail Effects

The effects of afterbody boattailing on the aerodynamic characteristics in pitch of a body without the sting are also shown in figure 4, and a summary of corresponding sting-off characteristics is presented in figure 5. As would be expected from geometrical consideration of the bodies, the cylindrical afterbody configuration (I-1) has the greatest lift-curve slope and is the most stable of the test configurations throughout the Mach number range of the test.

There is little difference in C_{L_α} and C_{m_α} between the closed afterbody configuration (I-4) and the $\frac{d}{d_{max}} = 0.33$ configuration (I-3). The $\frac{d}{d_{max}} = 0.67$ configuration (I-2) has intermediate values of C_{L_α} and C_{m_α} to those for the closed and cylindrical afterbody configurations except at Mach numbers of 2.50 and 2.87 where C_{m_α} for all of the boattail configurations is essentially the same.

The effect of afterbody boattail on drag coefficient (adjusted for chamber drag coefficient) is appreciable throughout the Mach number range of the tests with $C_{D,min}$ progressively increasing from the cylindrical afterbody configuration (I-1) to the fully closed configuration (I-4). It is therefore apparent that a wind-tunnel model that has its afterbody appreciably altered to accommodate a rear-mounted sting support will produce different drag characteristics than those which would be obtained from a true representation of an airplane with a closed afterbody.

The effect of afterbody boattail on base-pressure coefficient is presented in figure 6 which shows a decrease in the base-pressure coefficient with decrease in d/d_{max} for both the 14.50-inch- and the 19.00-inch-long afterbody configurations. These results are in general agreement with the results of reference 2. The decrease in C_p with decrease in d/d_{max} appears, within the scope of the present paper, to be independent of afterbody length.

With respect to base pressures, it should be noted (fig. 3) that there is, in general, little variation in base-pressure coefficient within the angle-of-attack range presented. The largest variations are realized with the cylindrical afterbodies (I-1 and II-1) at the lower Mach numbers of these tests.

Afterbody Camber Effects

The effects of afterbody camber on aerodynamic characteristics in pitch are presented in figure 7 and summarized in figure 8. Positive camber leads to increases in stability level, in lift-curve slope, and in minimum drag coefficient (see fig. 8). Further, a positive increment in $C_{L,o}$ is produced by the positive camber, and perhaps of more significance, is the substantial decrease in $C_{m,o}$ which indicates that negative afterbody camber should provide positive increments of $C_{m,o}$ that would relieve the trimming requirements.

The aerodynamic characteristics of a symmetrical conical afterbody configuration (I-7) are also shown in figure 7 and are compared in summary form with the symmetrical ogive afterbody configuration (I-4) in figure 9. There are no large differences in C_{L_α} or $C_{D,min}$ between these configurations; however, the conical afterbody configuration produces a slightly lower C_{m_α} than does the ogive afterbody configuration.

Effect of Afterbody Length

Results of tests on the basic forebody configuration with lengthened afterbodies are presented in figure 10. The same general effects of sting and afterbody boattailing noted on the aerodynamic characteristics of the shorter afterbody configurations are observed on the longer configurations.

A comparison of the results presented in figures 4 and 10 indicates that the aerodynamic characteristics in pitch for the 14.50-inch and the 19.00-inch afterbody configurations differ only superficially except for the minimum drag-coefficient values of the cylindrical afterbody configurations. For these configurations, the longer model has the greater $C_{D,min}$, which is obviously due to an increase in wetted area over that for the shorter model. For the boattail configuration (II-4 with respect to I-4) it would appear that the drag coefficient due to added wetted area is compensated for by a decrease in boattail angle.

CONCLUSIONS

Tests of afterbody configurations with changes in the diameter of the rear-mounted sting, afterbody boattailing, camber, and length at Mach numbers from 1.50 to 2.86 lead to the following conclusions:

1. Wind-tunnel models with afterbodies appreciably altered to accommodate a rear-mounted sting-support system will produce different drag characteristics than those which would be obtained from true representations of the aircraft with closed afterbodies.

2. Negative afterbody camber may be of significant benefit in minimizing the trim performance penalty of airplanes.

3. There is little effect of sting diameter on the aerodynamic characteristics in pitch of wind-tunnel models that have turbulent flow over their length.

4. There is, in general, little variation in base-pressure coefficient with angle of attack from -4° to 4°.

Langley Research Center,
National Aeronautics and Space Administration,
Langley Station, Hampton, Va., August 30, 1963.

REFERENCES

1. Perkins, Edward W.: Experimental Investigation of the Effects of Support Interference on the Drag of Bodies of Revolution at a Mach Number of 1.5. NACA TN 2292, 1951. (Supersedes NACA RM A8B05.)

2. Love, Eugene S.: Base Pressure at Supersonic Speeds on Two-Dimensional Airfoils and on Bodies of Revolution With and Without Fins Having Turbulent Boundary Layers. NACA TN 3819, 1957. (Supersedes NACA RM L53C02.)

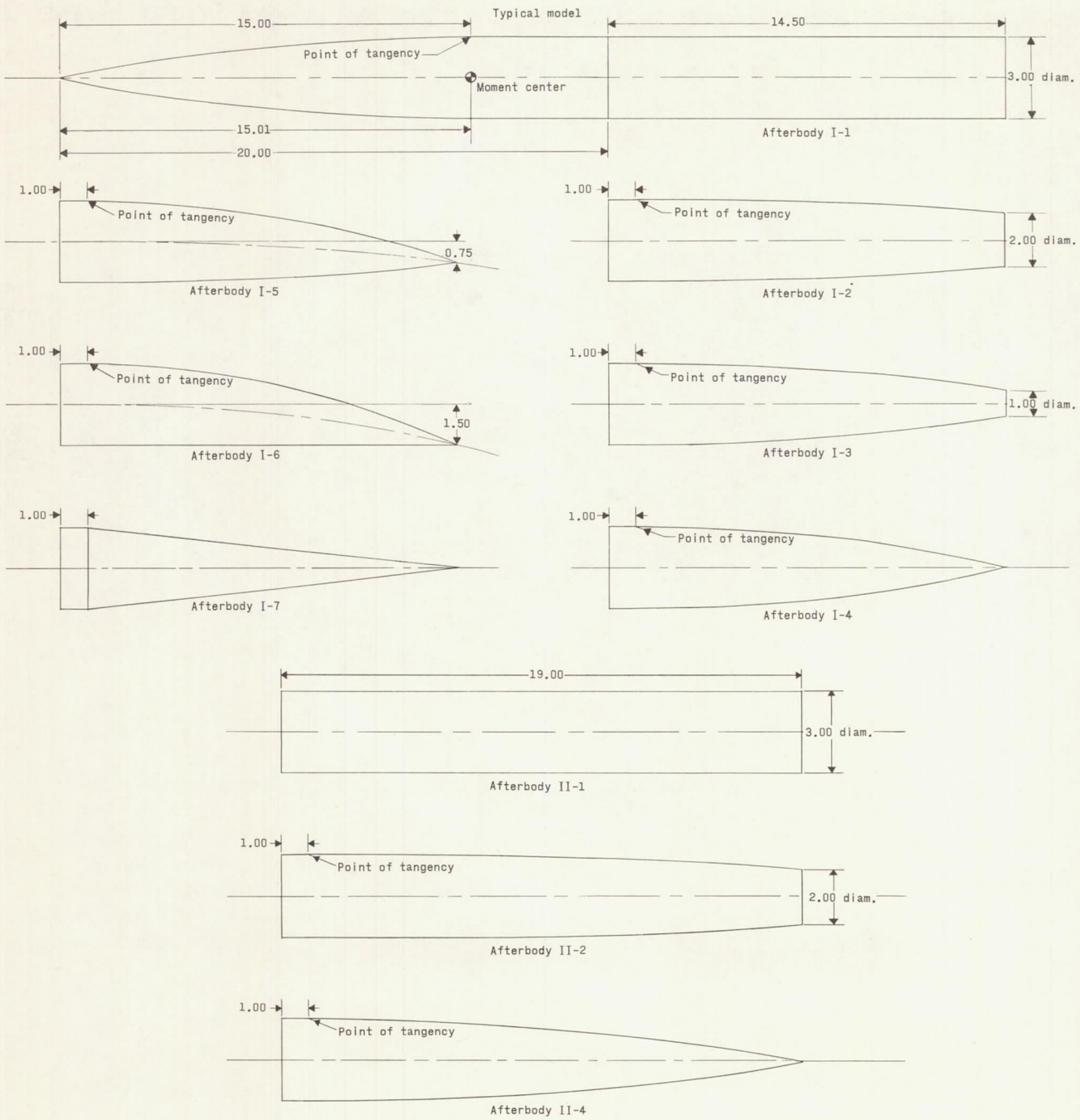

Figure 1.- Dimensional details of test configurations. All dimensions are in inches.

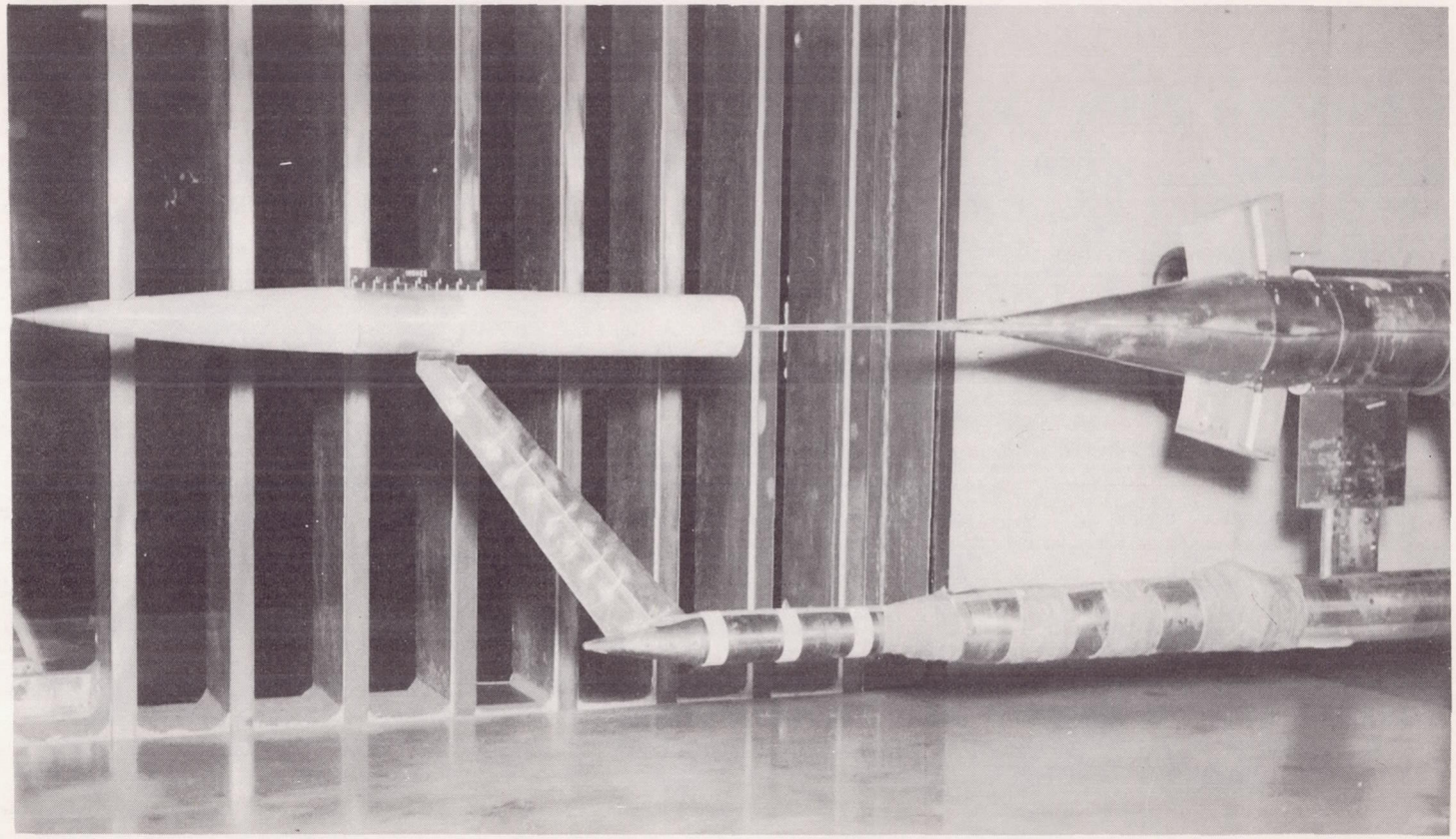

Figure 2.- Photograph of support strut with model I-1. L-62-9538

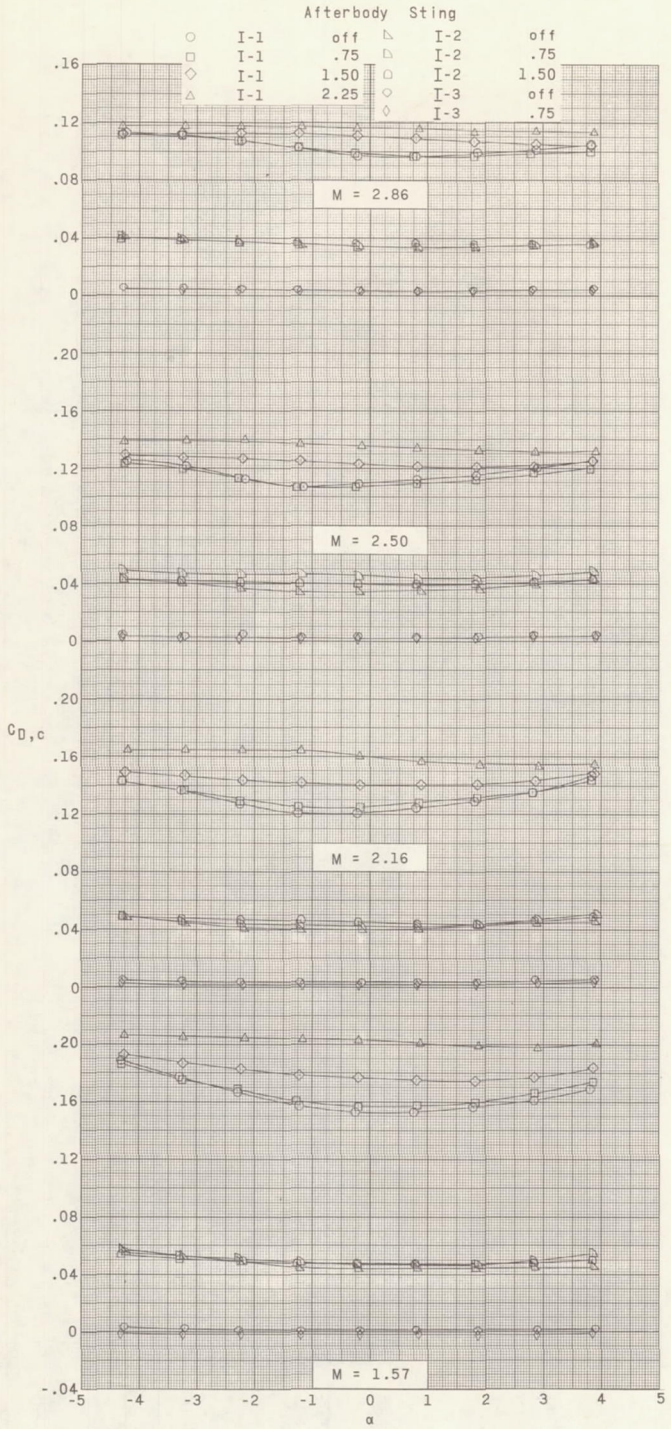

(a) 14.50-inch afterbodies.

Figure 3.- Variation of chamber drag coefficient with angle of attack.

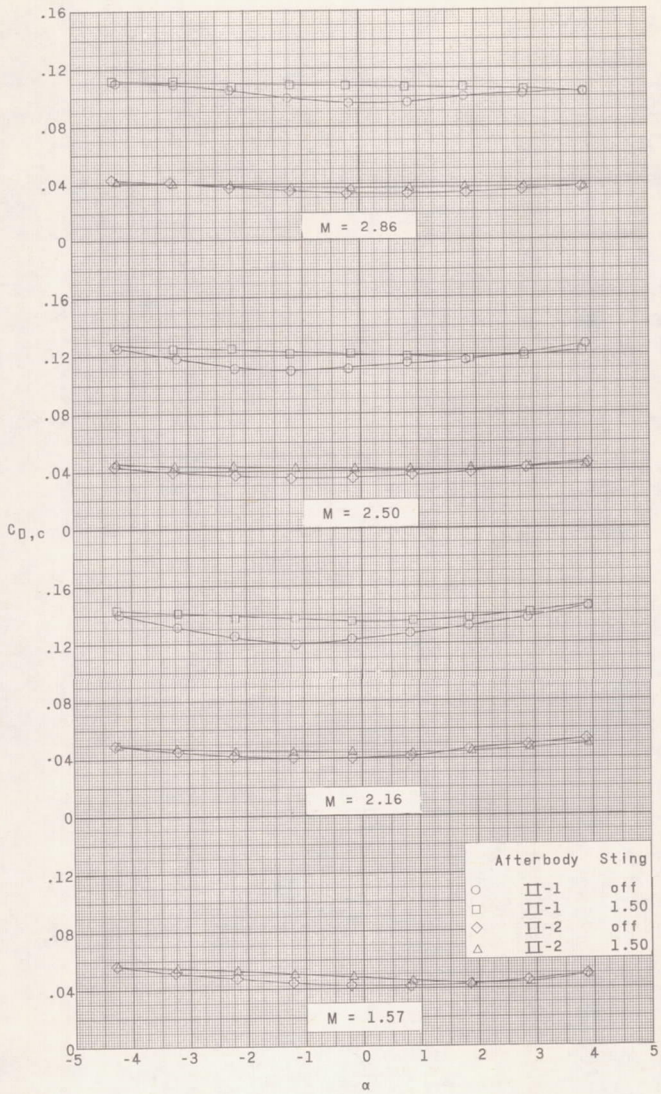

(b) 19.00-inch afterbodies.

Figure 3.- Concluded.

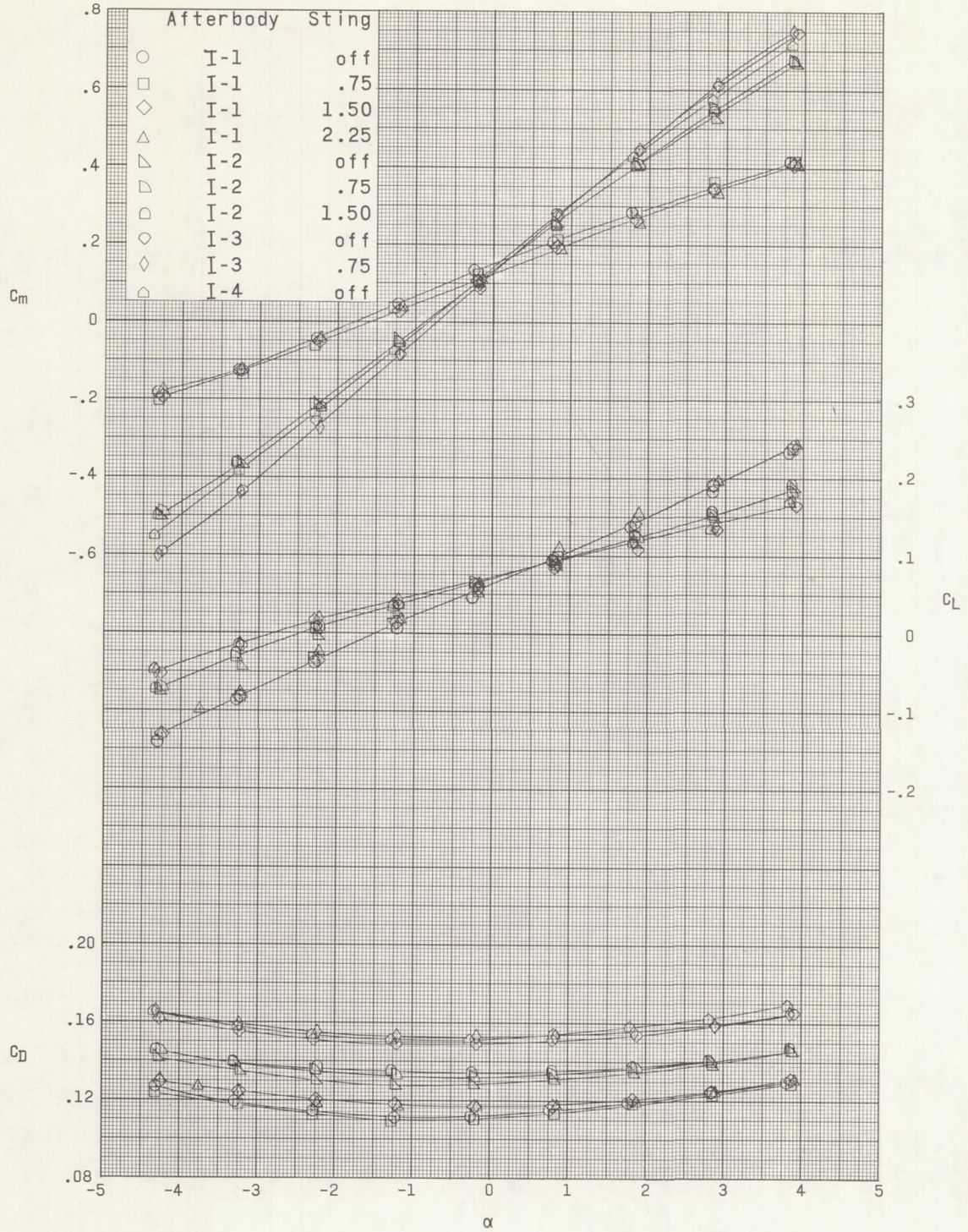

(a) M = 1.57.

Figure 4.- Effect of sting diameter and afterbody boattailing on aerodynamic characteristics in pitch.

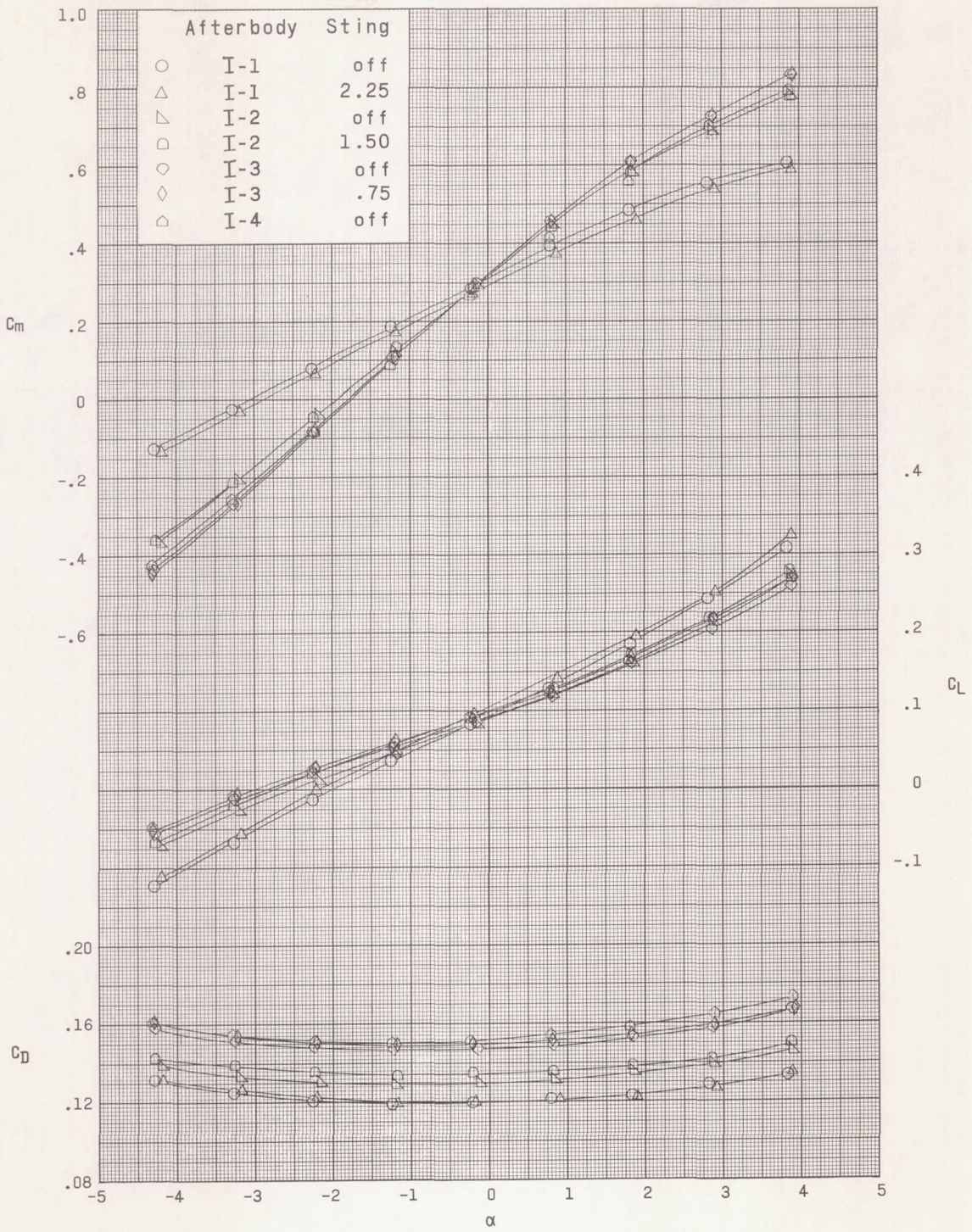

(b) M = 2.16.

Figure 4.- Continued.

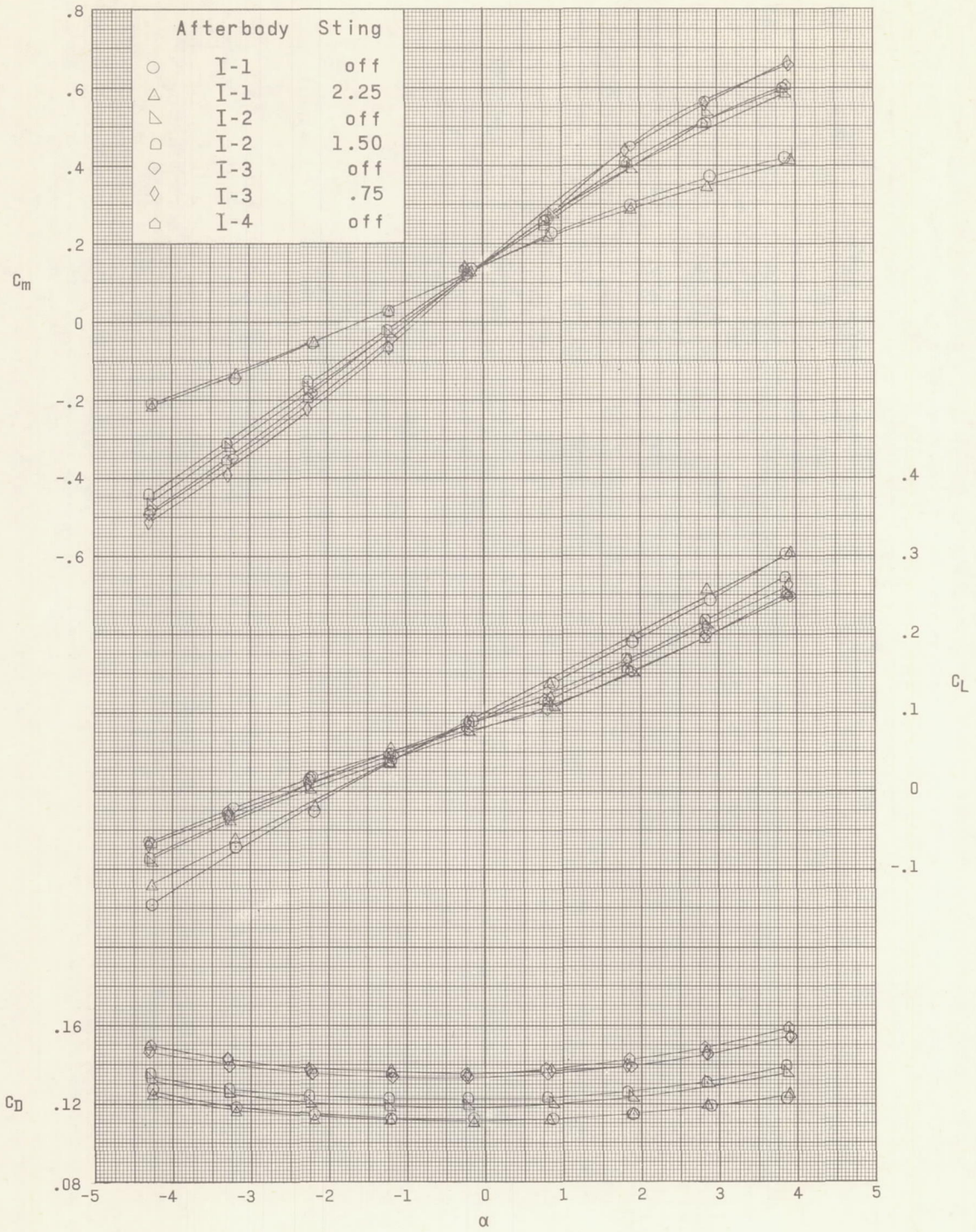

(c) M = 2.50.

Figure 4.- Continued.

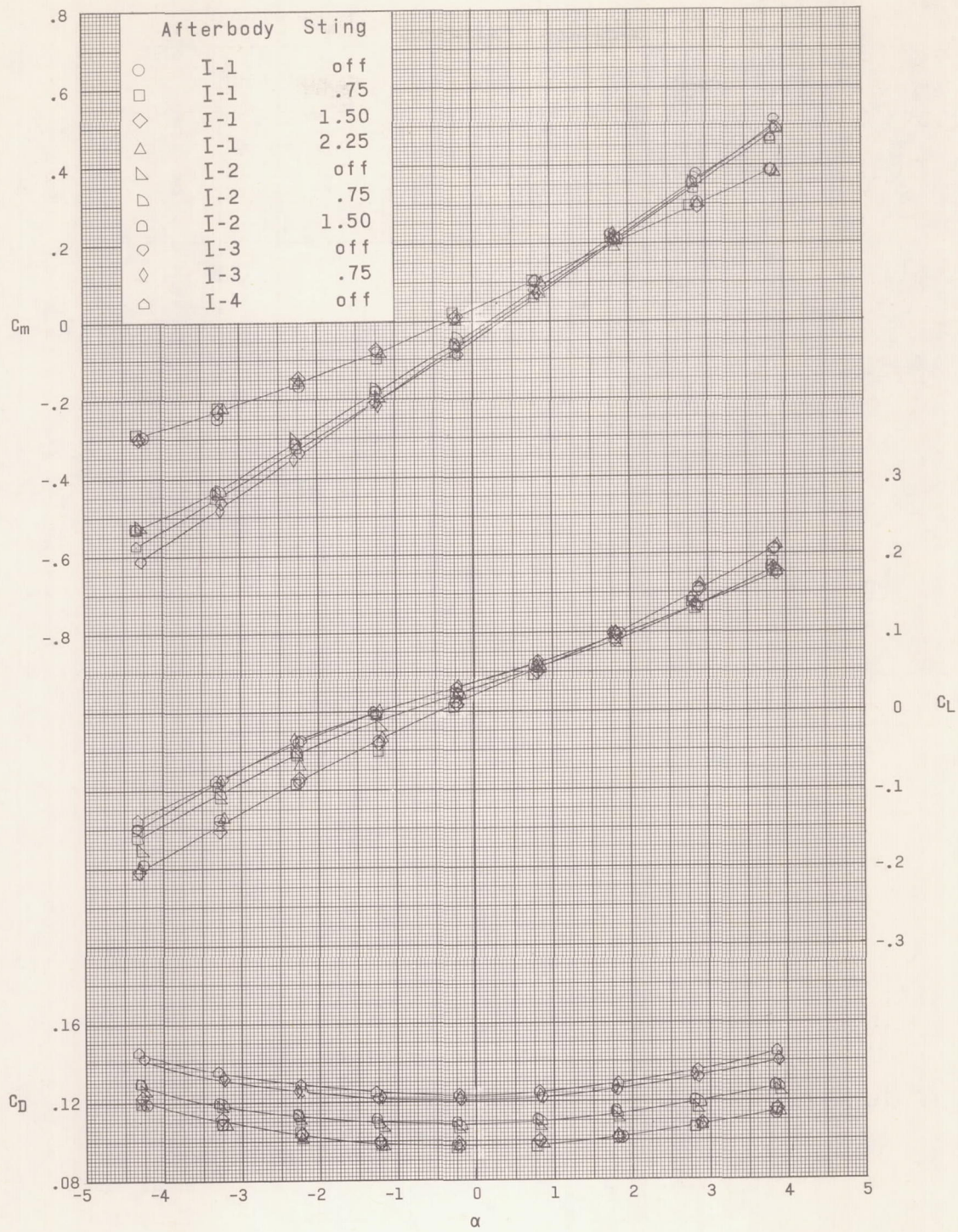

(d) M = 2.86.

Figure 4.- Concluded.

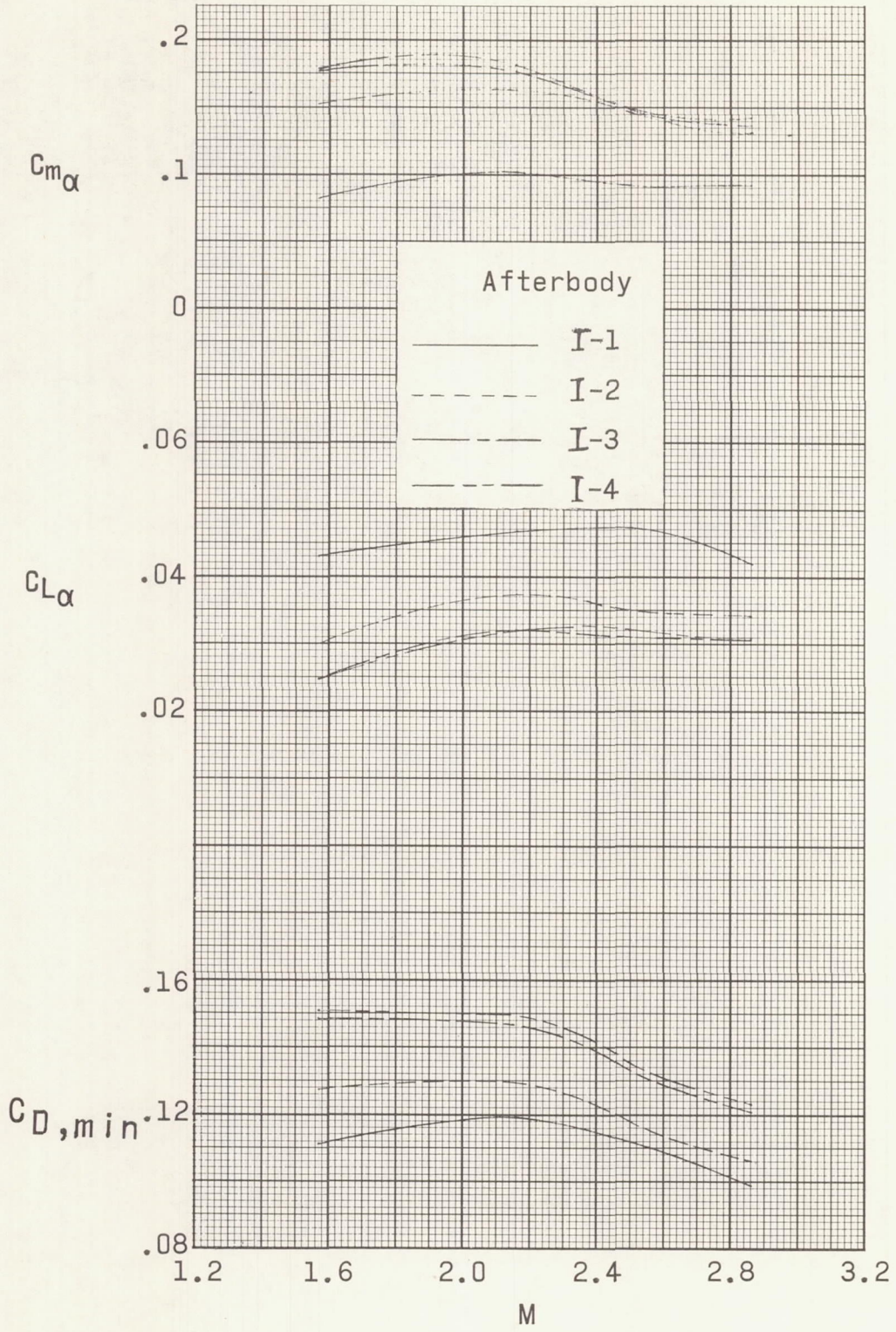

Figure 5.- Summary of afterbody boattail effects in pitch with the sting off.

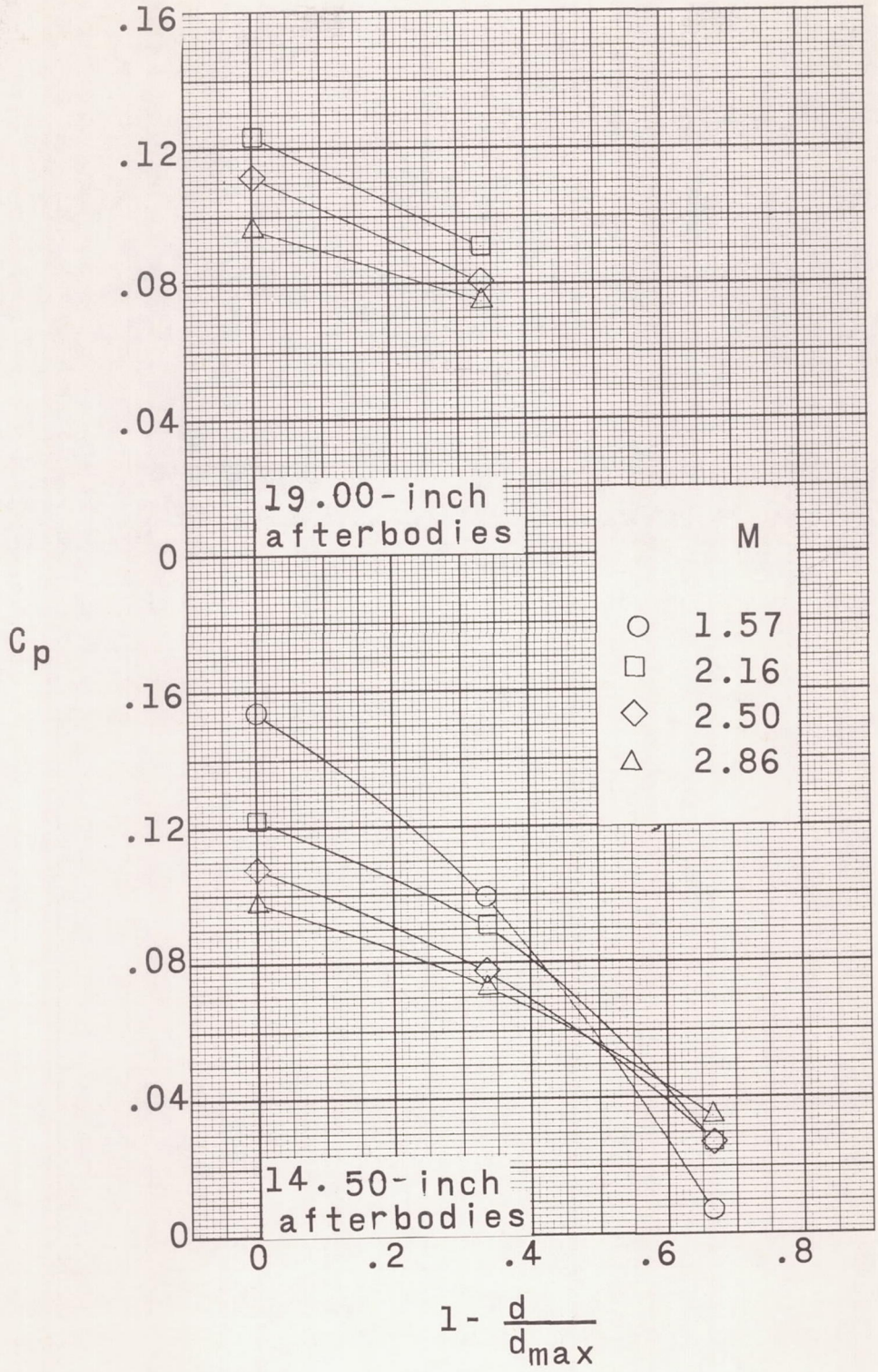

Figure 6.- The effect of afterbody boattail on base-pressure coefficients.

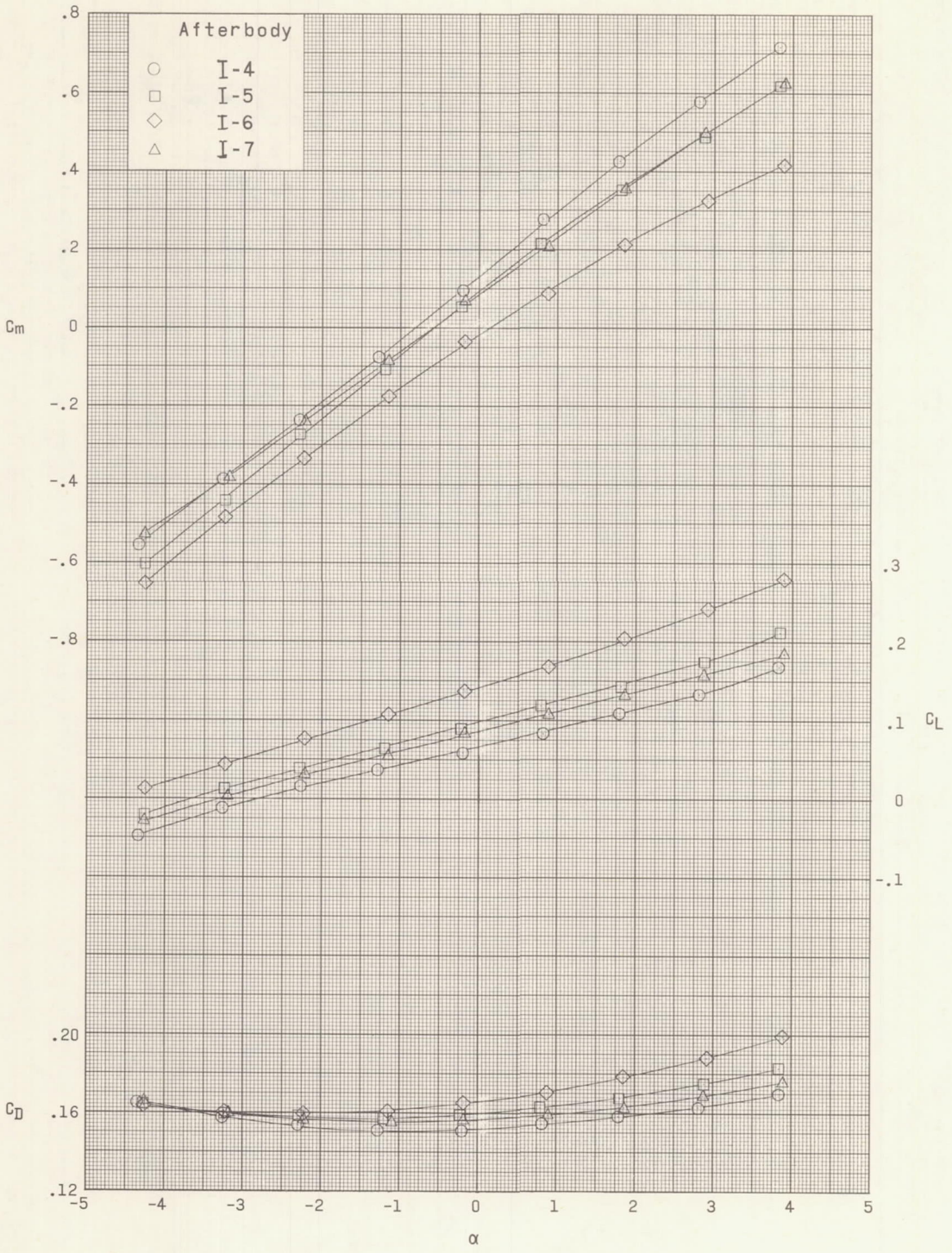

(a) M = 1.57.

Figure 7.- Effect of afterbody camber on aerodynamic characteristics in pitch.

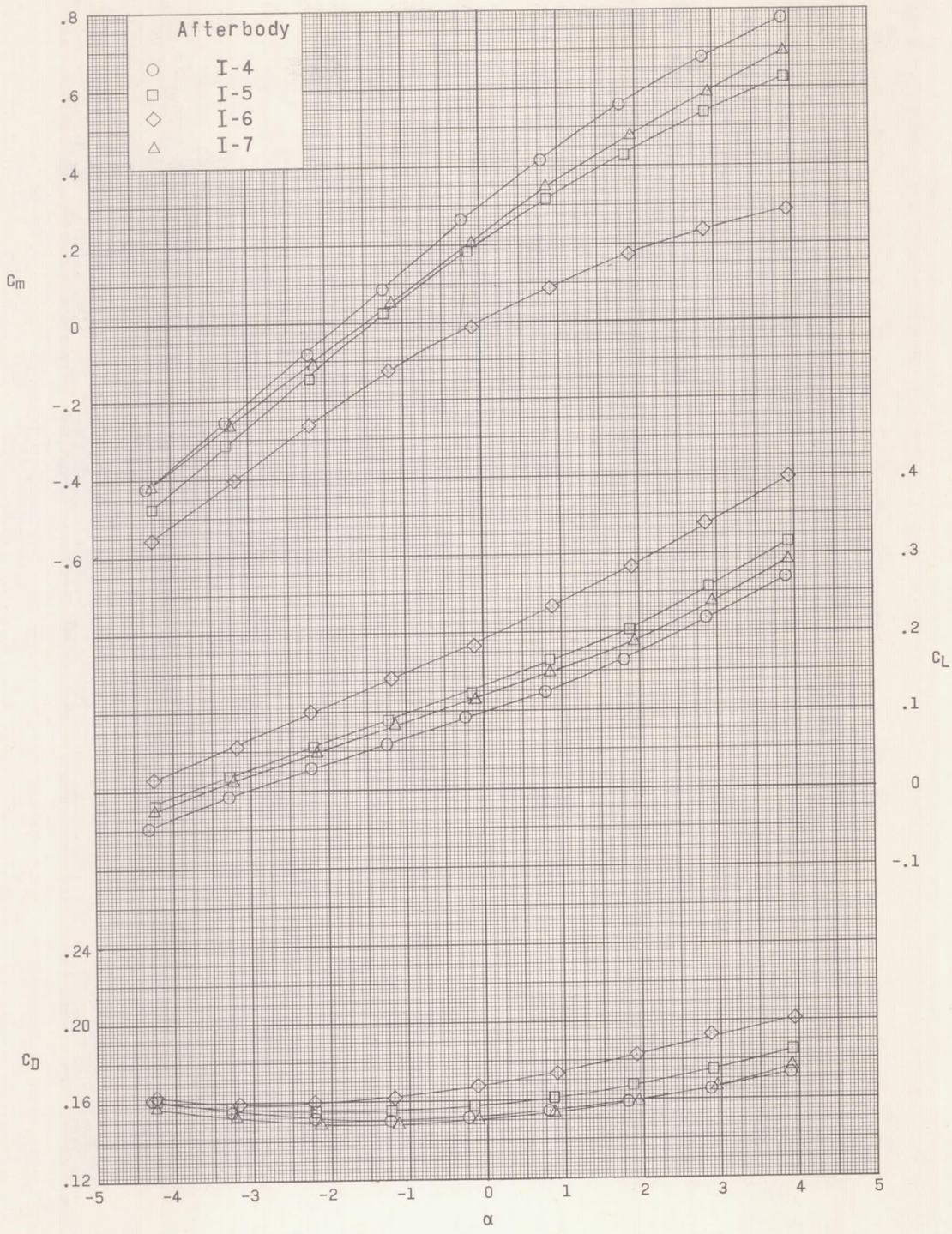

(b) M = 2.16.

Figure 7.- Continued.

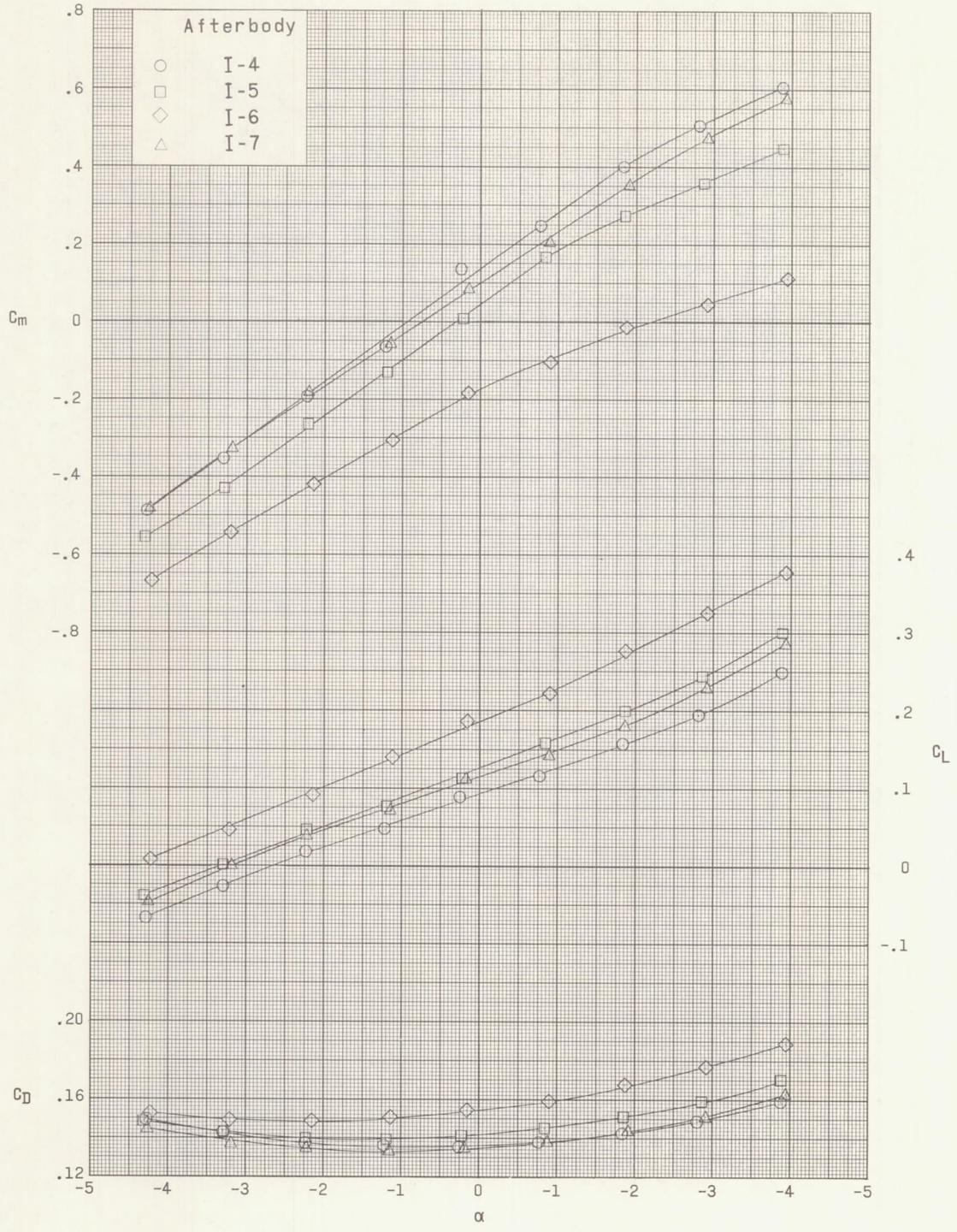

(c) M = 2.50.

Figure 7.- Continued.

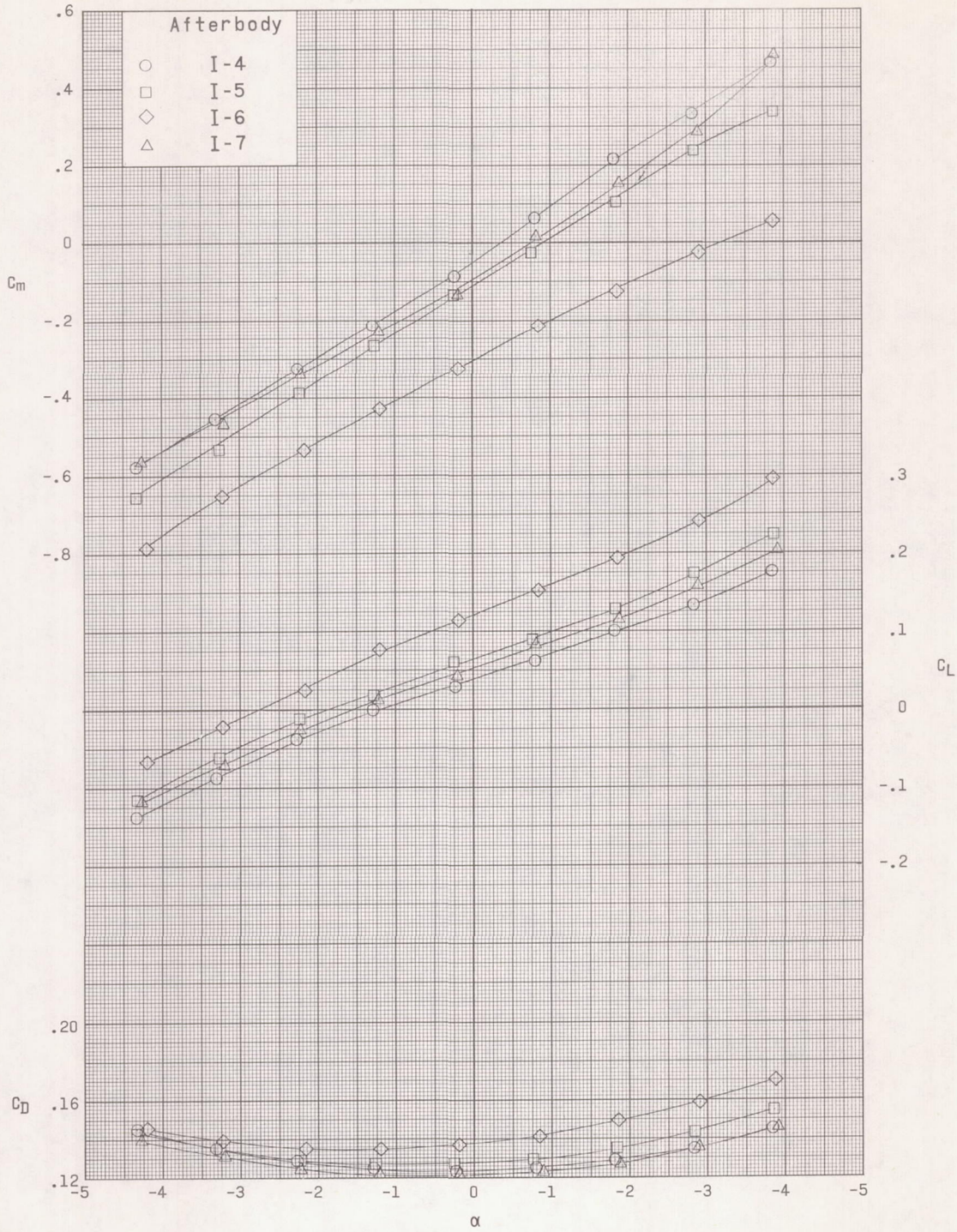

(d) M = 2.86.

Figure 7.- Concluded.

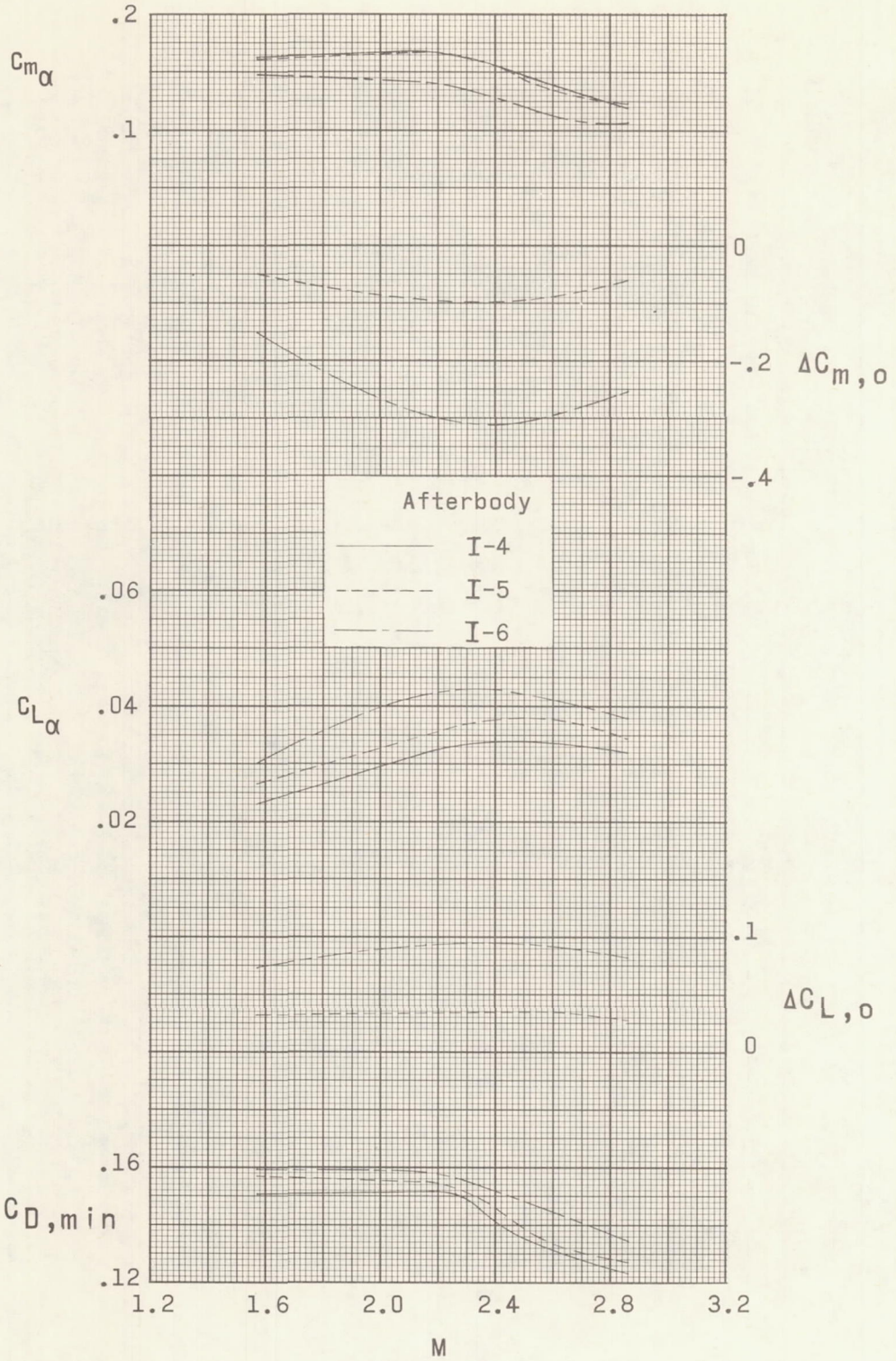

Figure 8.- Summary of afterbody camber effects.

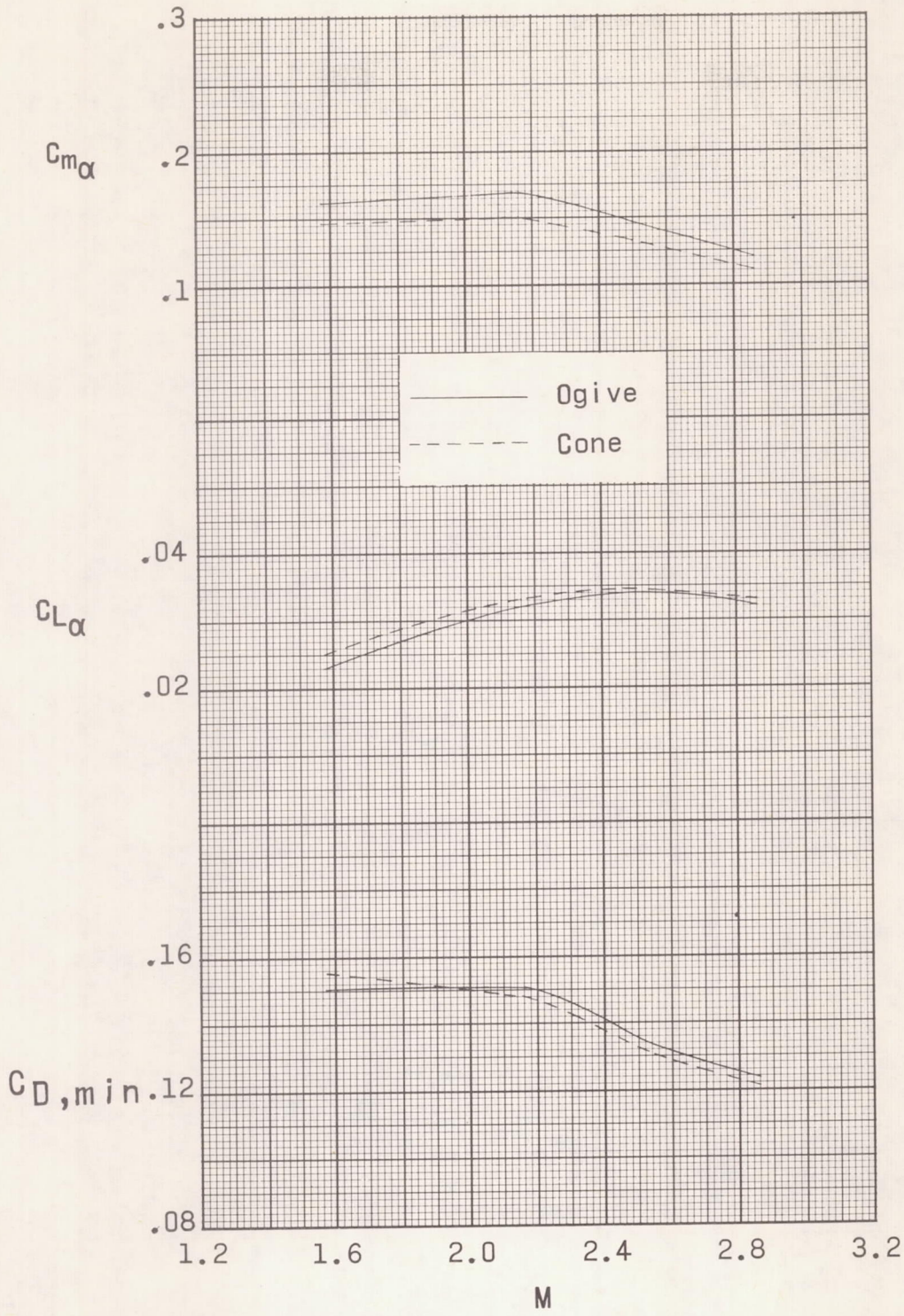

Figure 9.- Comparison of longitudinal parameters for ogive afterbody and conical afterbody configurations.

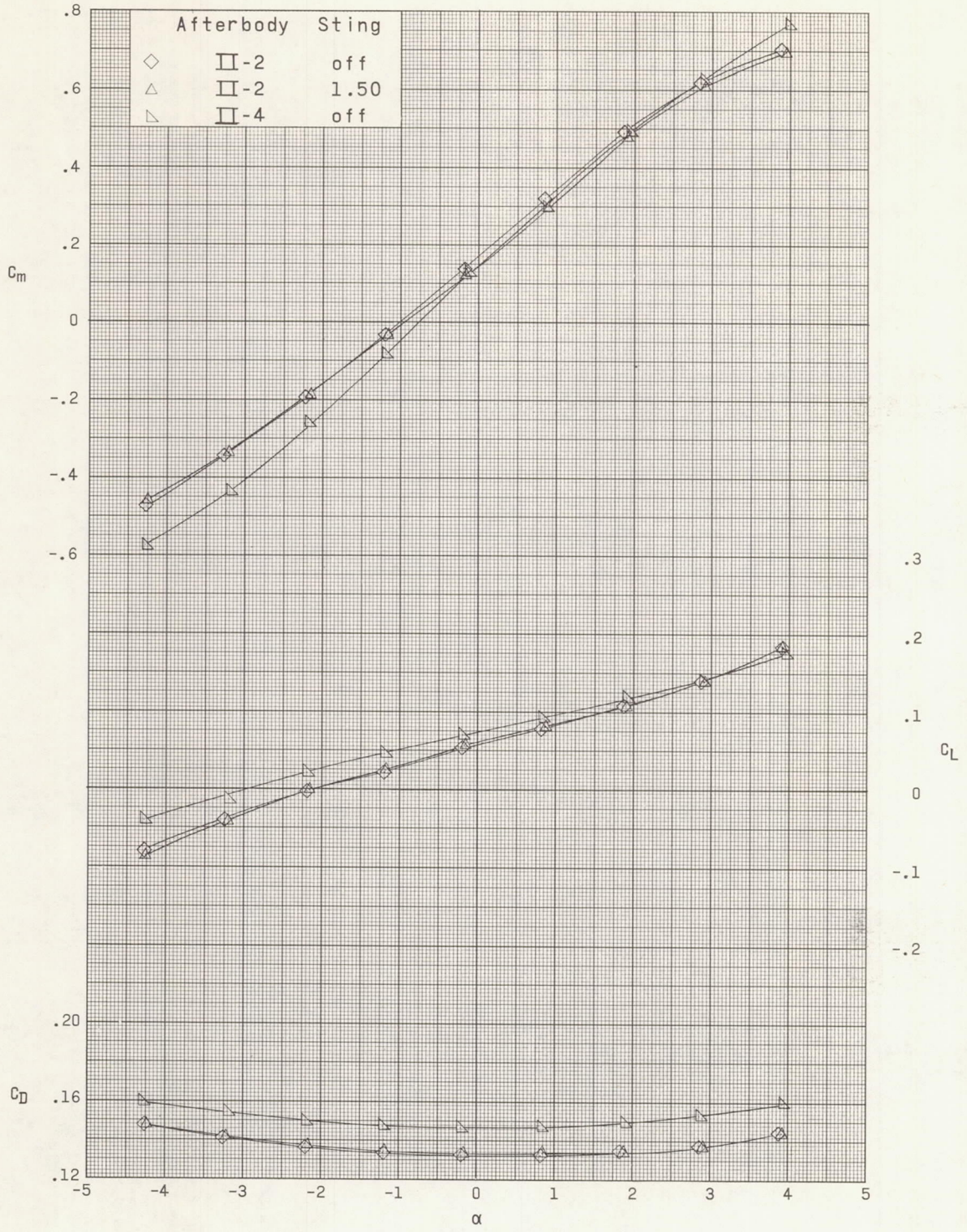

(a) M = 1.57.

Figure 10.- Aerodynamic characteristics in pitch of configuration with lengthened afterbody.

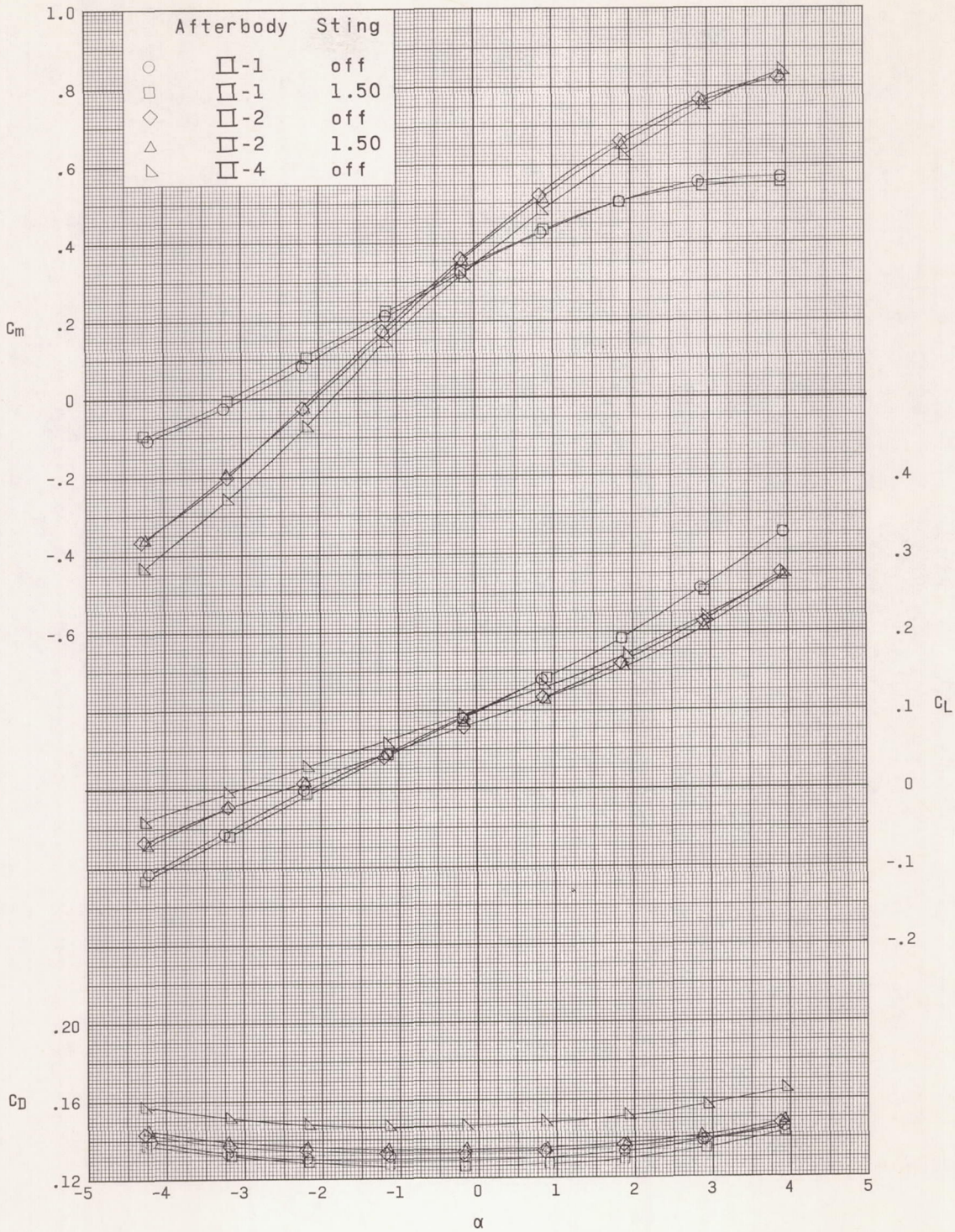

(b) M = 2.16.

Figure 10.- Continued.

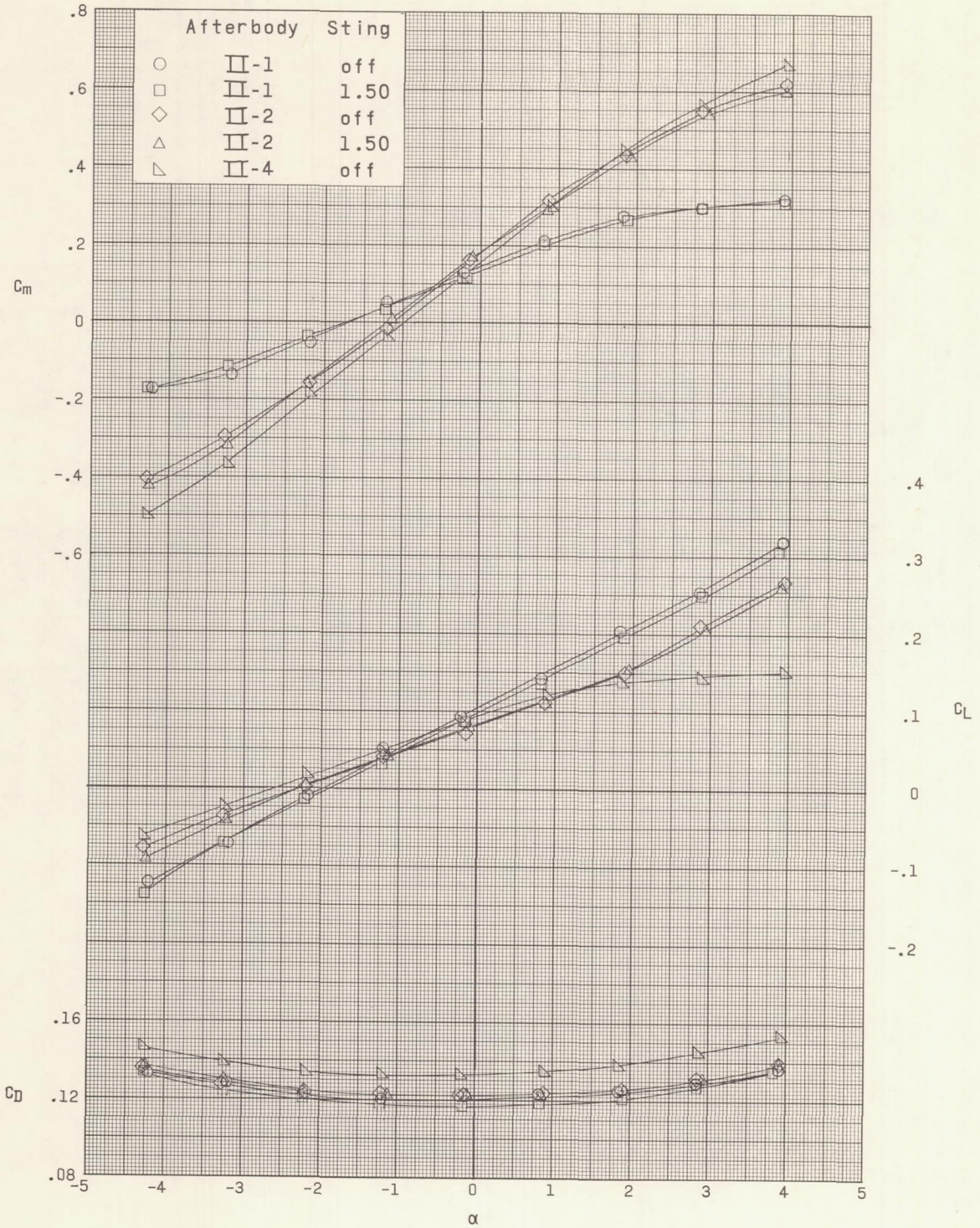

(c) M = 2.50.

Figure 10.- Continued.

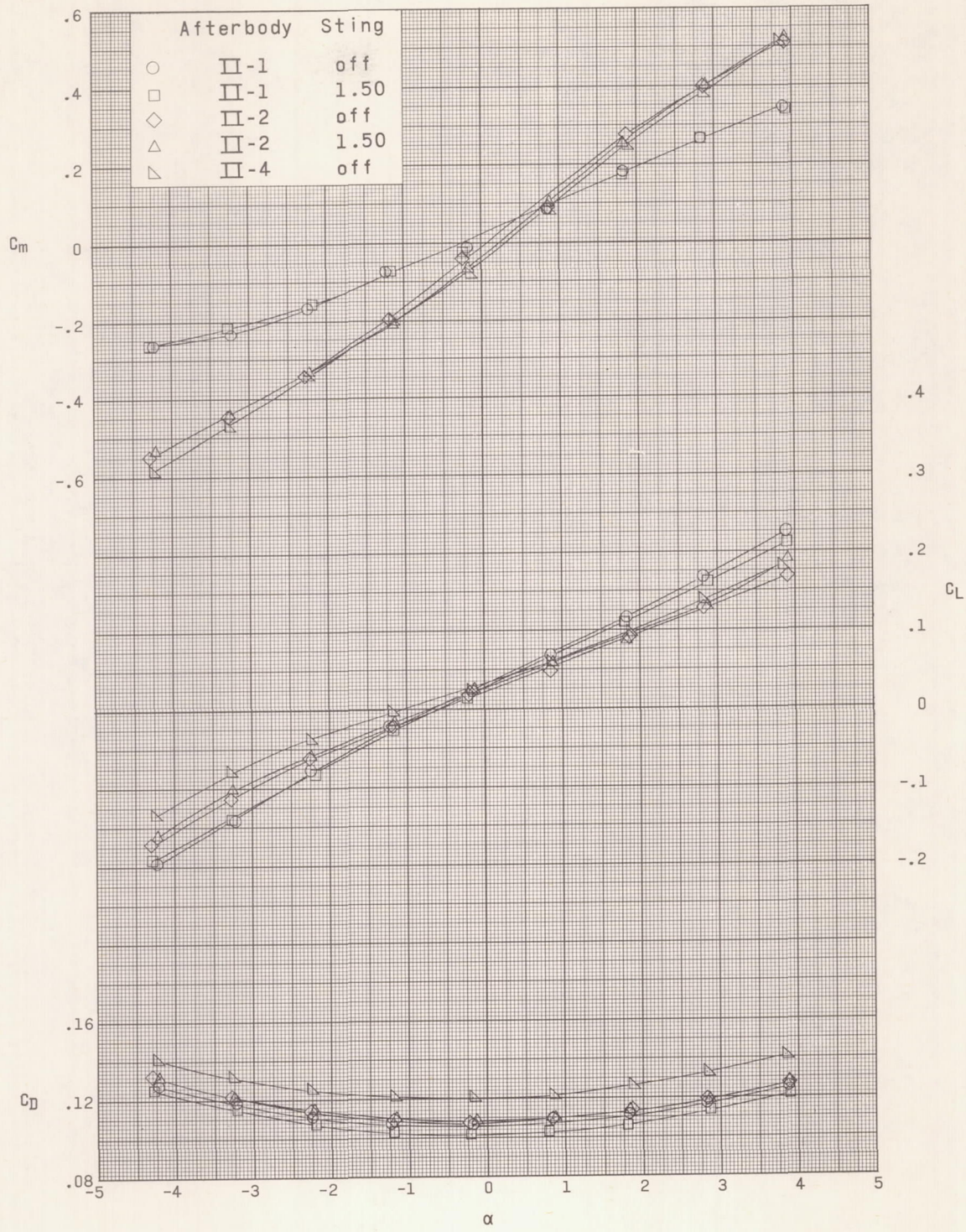

(d) M = 2.86.

Figure 10.- Concluded.